Numerical Analysis for Damping Responses of Automotive Rear Seat Structure with Leather Sheet Using FEM Described by Biot Type Poroelastic Material Model

Chihiro Kamio[1,a], Takao Yamaguchi[1,b,*], Masashi Fujimoto[1], Koki Yamaguchi[1], and Shinichi Maruyama[1,c]

[1]Gunma University, 1-5-1 Tenjin-cho, Kiryu, Gunma, 376-8515 Japan

* Corresponding author

[a]<chihiro.kamio@gunma-u.ac.jp>, [b]<yamagme3@gunma-u.ac.jp>,

[c]<maruyama@gunma-u.ac.jp>

Keywords: damping, Biot type poroelastic material, seat structure, finite element method

Abstract. This report describes damping response analysis of the rear seat structure for automobiles by experiment and FEM proposed by Yamaguchi. For the rear seats, there exist steel panels backside of seat foams, while there are metal frames instead of steel panels for front seats, which we reported previously. The seat structure is modeled by three -dimensional finite element using Biot type porous material. Both resin skeleton and internal air are able to propagate waves in the Biot type material (i.e. poroelastic material). The models of using analysis are a steel panel without porous material, a steel panel with a porous material, a steel panel with a porous material and a leather sheet. Using them, damping responses and dynamic deformations are verified by the experiment. And effects of leather sheets on the responses are investigated.

1. Introduction

In this study, we analyzed the damping response of the seat, which is the largest component of an automobile interior structure. It is known that seats have a significant affection on interior noise during driving cars, and their dynamic characteristics is essential for improving the accuracy of the computer aided engineering (CAE) of the entire vehicle body, which is performed before prototyping. The structure of an automobile seat is composed of metal frames (in front seats), metal panels (in rear seats), a porous urethane foam that acts as a cushion, and skin materials such as clothes or leather sheets. Thus, automotive interior structures, including seats, are composed of a mixture of elastic, viscoelastic, porous, and gas materials [6]-[8]. And then, vibration and acoustic analysis must take these into account.

In our previous work [3], we investigated the vibration characteristics of the front seats, in which there exists a frame structure backside of the poroelastic urethane foam. In our past works [5],[7], we proposed a new fast calculation method named as MSKE method to compute modal damping. Using this method, we clarify the effects of sound bridge phenomena for the double walled structures (i.e. a porous layer sandwiched by double solid walls) [6]. As for our works [5]-[7], we consider characteristics of the only air phase inside the porous material under condition that the rigidity of the resin skeleton can be neglected because of its flexible resin skeleton. This model is effective for very light and flexible materials like fluffy cottons. For the urethane foam in the seats, we cannot neglect the rigidity of its resin skeletons. Therefore, we have to introduce the porpelastic Biot model.

In this study, a simple FEM model of the rear seat structure was created to investigate. As for the rear seats, there are steel panels backside of seat foams, while there exist metal frames in place of steel panels for front seats, which we reported previously [3]. The models used in the analysis are a steel panel without porous material, a steel panel with a porous material, a steel panel with a porous material and a leather sheet. The damping response analysis was numerically carried out using three-dimensional finite elements that take into account the coupling of damping including poroelastic materials, as proposed by Yamaguchi et al. [3]. And effects of leather sheets on the responses are investigated. In this study, we applied Biot model [1] used in FEM for porous foams. We modified the models proposed by Bolton et al. [2]. In our investigation, we adopted the particle displacement $\{U\}$ of the air in foams and the displacement $\{u\}$ of the resin skeleton in foams as unknowns. Bolton used relative displacement $\{u\}-\{U\}$ and $\{U\}$ as unknowns. Attala [4] selected sound pressure $\{P\}$ and $\{u\}$ as unknowns. By selection of our unknowns, we can visualize deformations in both $\{u\}$ and $\{U\}$.

2. Analytical Model

2.1 Discretization of vibration field in both resin skeleton and internal air for poroelastic material

Biot model is an elastic porous material model (i.e. proelastic material model) that takes into account the elastic deformation of the resin skeleton (treated as a viscoelastic material) in addition to the internal air [1]-[4].

If we define the particle displacement vector $\{U\}=\{U_x,U_y,U_z\}^T$ of the internal air and the skeleton displacement vector $\{u\}=\{u_x,u_y,u_z\}^T$, the equation of motion becomes for internal air:

$$-\omega^2(\rho_{21}u_x+\rho_{22}U_x)+j\omega b(U_x-u_x)=-\Omega(\partial p/\partial x) \tag{1}$$

$$-\omega^2(\rho_{21}u_y+\rho_{22}U_y)+j\omega b(U_y-u_y)=-\Omega(\partial p/\partial y) \tag{2}$$

$$-\omega^2(\rho_{21}u_z+\rho_{22}U_z)+j\omega b(U_z-u_z)=-\Omega(\partial p/\partial y) \tag{3}$$

and for skeleton (viscoelastic material):

$$-\omega^2(\rho_{11}u_x+\rho_{12}U_x)+j\omega b(u_x-U_x)=(\partial\sigma_x/\partial x)+\left(\partial\tau_{xy}/\partial y\right)+(\partial\tau_{xz}/\partial z) \tag{4}$$

$$-\omega^2(\rho_{11}u_y+\rho_{12}U_y)+j\omega b(u_y-U_y)=\left(\partial\sigma_y/\partial y\right)+\left(\partial\tau_{yz}/\partial z\right)+\left(\partial\tau_{yx}/\partial x\right) \tag{5}$$

$$-\omega^2(\rho_{11}u_z+\rho_{12}U_z)+j\omega b(u_z-U_z)=(\partial\sigma_z/\partial z)+(\partial\tau_{zx}/\partial x)+(\partial\tau_{zy}/\partial y) \tag{6}$$

Where, $\rho_{21}=-\rho_a$, $\rho_a=\rho_f(s-1)$, s is the tortuosity, $\rho_f=\rho_0\Omega$, ρ_0 is the mass density of the air, Ω is the porosity. $\rho_{22}=\rho_f+\rho_a$. And $b=\Omega r$ is the flow resistance. $\rho_{11}=\rho_s+\rho_a$, $\rho_{12}=-\rho_a$, $\rho_s=\rho_1(1-\Omega)$ and $\rho_1$is the mass density of the resin skeleton. σ_x is the normal stresses in x direction, respectively. $\tau_{xy}$is the shear stress.

The second term on the left-hand side of equations (1) to (6) represents the viscous resistance caused by internal friction when air escapes through the pores, which acts on the relative velocity between the internal air and the skeleton.

The formula for compressing the internal air is as follows:

$$-\Omega p = Q_m div\{u\} + E_m div\{U\} \tag{7}$$

Where, $E_m = \Omega E^*$, $E^*$is the bulk modulus of elasticity for the internal air. $Q_m = (1-\Omega)E^*$ is the coupling modulus of elasticity. The first term on the right-hand side indicates that the volume expansion rate $div\{u\}$ of the skeleton affects the spring characteristics of the internal air (the relationship between pressure p and volume expansion rate $div\{U\}$). These are complex numbers to take hysteresis damping into account.

The relationship between stress and strain in the skeleton (viscoelastic material) is given by the following equation.

$$\sigma_x = 2G_s^*(\partial u_x/\partial x) + A_s^* div\{u\} + Q_m div\{U\} \tag{8}$$

$$\sigma_y = 2G_s^*(\partial u_y/\partial y) + A_s^* div\{u\} + Q_m div\{U\} \tag{9}$$

$$\sigma_z = 2G_s^*(\partial u_z/\partial z) + A_s^* div\{u\} + Q_m div\{U\} \tag{10}$$

$$\tau_{xy} = \tau_{yx} = G_s^*((\partial u_x/\partial y) + (\partial u_y/\partial x)) \tag{11}$$

$$\tau_{yz} = \tau_{zy} = G_s^*((\partial u_y/\partial z) + (\partial u_z/\partial y) \tag{12}$$

$$\tau_{zx} = \tau_{xz} = G_s^*((\partial u_z/\partial x) + (\partial u_x/\partial z) \tag{13}$$

$G_s^* = E_s(1+j\eta_s)/2(1+\nu_s)$, $A_s^* = E_s\nu_s(1+j\eta_s)/((1+\nu_s)(1+2\nu_s))$. G_s^* is the shear modulus of elasticity of the resin skeleton. E_s, η_s and ν_s are the storage modulus of elasticity, the material loss factor and Poisson's ratio, respectively. The stress in the skeleton is also affected by the volume change of the internal air in the terms $Q_m div\{U\}$. G_s^* and A_s^* are complex numbers because they take into account the vibration suppression effect of the skeleton's hysteresis damping.

Eliminating pressure p and rearranging equations (1) to (13), we obtain simultaneous differential equations with the internal air particle displacement $\{U\}$ and the skeleton displacement $\{u\}$ as unknowns.

Next, the relationship between the internal air particle displacement $\{U\}$ within the element and the internal air particle displacement $\{U_e\}$ at the node is approximated using an interpolation function matrix $[N_U]^T$ as follows:

$$\{U\} = [N_U]^T\{U_e\} \tag{14}$$

The relationship between the displacement $\{u\}$ of the skeleton part within the element and the displacement $\{u_e\}$ at the node is similarly approximated using an interpolation function matrix $[N_u]^T$ as follows:

$$\{u\} = [N_u]^T\{u_e\} \tag{15}$$

Using equations (14) and (15), we apply the Galerkin method to the simultaneous differential equations for $\{U\}$ and $\{u\}$. Further summarizing this in a weak form yields the following discretized equations:

$$-\omega^2([M_{11}]\{u_e\}+[M_{12}]\{U_e\})+j\omega([C_{11}]\{u_e\}+[C_{12}]\{U_e\})+([K_{11}]\{u_e\}+[K_{12}]\{U_e\})=\{F_e\} \quad (16)$$

$$-\omega^2([M_{22}]\{U_e\}+[M_{21}]\{u_e\})+j\omega([C_{22}]\{U_e\}+[C_{21}]\{u_e\})+([K_{22}]\{U_e\}+[K_{21}]\{u_e\})=\{f_e\} \quad (17)$$

$$[M_{11}]=\iint_e \rho_{11}[N_u][N_u]^T dxdydz,\ [M_{12}]=\iint_e \rho_{12}[N_u][N_U]^T dxdydz,$$
$$[M_{21}]=\iint_e [N_U][N_u]^T dxdydz,\ [M_{22}]=\iint_e \rho_{22}[N_U][N_U]^T dxdydz,$$
$$[C_{11}]=\iint_e b[N_u][N_u]^T dxdydz,\quad [C_{12}]=-\iint_e b[N_u][N_U]^T dxdydz,$$
$$[C_{21}]=-\iint_e b[N_U][N_u]^T dxdydz,\quad [C_{22}]=\iint_e b[N_U][N_U]^T dxdydz,$$
$$[K_{11}]=\iint_e [B_u][D][B_u]^T dxdydz,\quad [K_{12}]=\iint_e Q_m[B_u][d][B_U]^T dxdydz,$$
$$[K_{21}]=\iint_e Q_m[B_U][d][B_u]^T dxdydz,$$
$$[K_{22}]=\iint_e E_m\{([N_U]/\partial x)([N_U]^T/\partial x)+([N_U]/\partial y)([N_U]^T/\partial y+([N_U]/\partial z)([N_U]^T/\partial z)\}dxdydz$$

Where, $[D]$ is a matrix consisting of the Poisson 's ratio ν_s and complex shear modulus G_s^* of the skeleton. $[B_u]=[L][N_u]^T$, and $[B_U]=[L][N_U]^T$, $[L]$ is a matrix consisting of spatial derivatives. $[d]$ is defined as follows.

$$[d]=\begin{bmatrix}1&1&1&0&0&0\\1&1&1&0&0&0\\1&1&1&0&0&0\\0&0&0&0&0&0\\0&0&0&0&0&0\\0&0&0&0&0&0\end{bmatrix}$$

We introduce $\{f_e\}$ and $\{F\}$ as external force vectors for acoustical input and dynamic load, respectively. When, the angular frequency ω and $\{f_e\}$ and $\{F\}$ are given as known quantities, equations (16) and (17) become complex simultaneous linear equations for $\{u_e\}$ and $\{U_e\}$. A constant strain hexahedral element [9] was used as the element corresponding to the poroelastic material.

2.2 Discretization of vibration fields related to solids

The vibration field of the solid is discretized using ordinary linear finite elements, assuming small amplitudes. For viscoelastic materials, hysteresis damping is taken into account by treating Young's modulus as a complex elastic modulus. The elements corresponding to these solids are eight-node isoparametric hexahedral elements that take into account the non-conforming modes [9].

2.3 Total system discretization equation

When the solid body and the resin skeleton in the foam are bonded, the displacement of the solid body and the displacement of the skeleton are continuous at the boundary. When the solid body and the elastic porous material skeleton are not bonded, the displacement of the solid body and the displacement of the skeleton have independent degrees of freedom at the boundary. On the other hand, at the boundary between the solid body and the air inside the elastic porous material, the particle displacement normal to the boundary and the displacement of the solid body in the same directions are continuous.

By taking the boundary conditions into consideration and superposing all elements of the field, the discretized equations of the entire system obtained become a complex simultaneous linear equation with displacements as unknowns when a periodic external force is applied. This was solved using the skyline method to calculate the response. We developed original numerical codes for abovementioned all calculations.

For road noise under normal driving conditions of cars, periodic components of the input are generally regarded as small sufficiently. However, though we adopted small input in our experiment to obtain more than 0.8 in coherence, it may be possible that nonlineality of the porous material affects the errors partially between the experiment and the calculation in this paper.

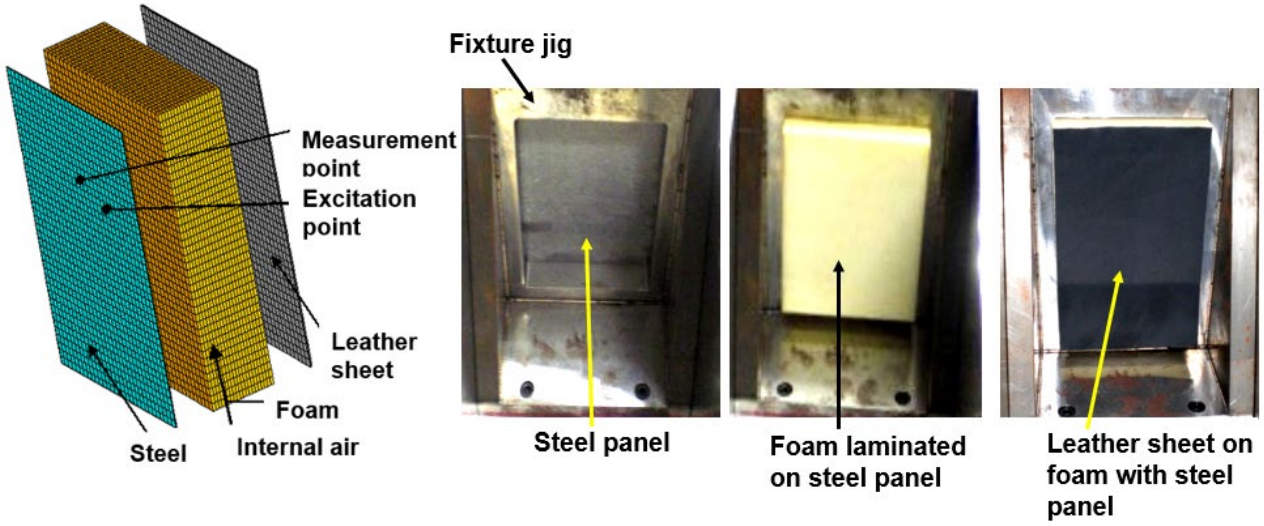

(a) FEM (b) Experiment

Fig.1. Model for FEM and Experiment

3. Analytical and Experimental Models

Figure 1 shows the analytical model used in the FEM and external view of the test specimens, respectively. The dimensions of the steel flat panel in the backrest of the automobile rear seat structure used in this report are 220[mm] in length, 150[mm] in width, and 0.8[mm] in thickness. A urethane foam is laminated on the steel plate. The dimensions of the urethane foam are 220[mm] in length, 150[mm] in width, and 50[mm] in thickness. A leather sheet is set on the urethane foam. And the dimensions of the leather sheet are 220[mm] in length, 150[mm] in width, and 1.5[mm] in thickness.

We adhered between the steel panel and foam with double-sided tape in the experiment, while in the FEM analysis, each node on the attachment surface was joined with complex spring elements. And we also adhered between the foam and leather in the same way. In our previous paper [2] on the condition that there exists a frame backside of the foam for the front seat, we used the same double-sided tape to adhere between the foam and the frame. We've already confirmed the calculation accuracy of responses using the same poroelastic urethane foam model and the same complex spring constants for the double-sided adhesive tape. In this previous investigation, we adopted the value of the complex spring constants to fit the response curves. Therefore, in this paper, we used the same complex spring constants for the double-sided adhesive tape because the FEM

model of the porous foam has the same mesh size and the same geometry as those in our previous paper.

The outer periphery of the steel panel was fixed with bolts, while in the FEM analysis model, only the outer periphery of the steel panel was fixed. The side of the foam, and the outer periphery of the leather sheet are set as free. The material properties of the steel panel, foam, and leather sheet are as follows:

For the steel panel, we set Young's modulus of 210 GPa, Poisson's ratio of 0.33, material loss factor of 1.00×10^{-3} [-], mass density of 7.8×10^{3} [kg/m ^{3}].

The foam had a storage modulus of 2.67×10^{-4} [GPa], a material loss factor of 0.106 [-], a Poisson's ratio of 0.40 [-], a porosity Ω of 0.97 [-], and a tortuosity s of 2.50 [-], flow resistivity r of 6.99[kNs/m^4], viscous characteristic length Λ of 0.00363 [mm]. The frequency dependency of flow resistance r is expressed using Λ[4]. And, the foam had thermal characteristic length Λ' of 0.169 [mm]. The frequency dependency of complex bulk modulus of elasticity E^* for the internal air is expressed using Λ' [4].

The leather sheet had a Young's modulus of 0.05[GPa], a Poisson's ratio of 0.45[-], a material loss factor of 0.1[-], and a mass density of 6.19×10^{2} [kg/m^3].

We compare among three conditions as follows: “steel panel only”, “steel panel with foam” and “steel panel with foam and leather sheet”.

4. Damping Response Analysis of Automotive Rear Seat Structures Subjected to Impact Excitation

In the experiment of hammering impact excitation, one point on the steel panel was excited by an impact hammer, and the acceleration was measured with an accelerometer placed at another point on the steel panel, and the inertance transfer function was calculated. The locations of the excitation point and observation point are shown in Fig.1(a). In the FEM analysis, the foam in the automotive rear seat structure was modeled as the Biot-type poroelastic material in which both the resin skeleton and the internal air can propagate waves. And the impact responses were calculated.

The results of the impact vibration responses using FEM and the experiment are shown in Fig.2. Figs. 3,4 and 5 show the deformation distribution at the frequencies corresponding to each peak in the response as shown in Fig.2. Note that the deformation distribution in the experiment only shows the deformation distribution of the steel panel.

In Fig.2, the experimental and calculated responses agree well except for the third peak with the leather sheet.

In Fig.2, the peak of the inertance transfer function and its resonance frequency are lower when foam is present than when there is only a steel panel. This result indicating that the foam has a vibration -suppressing effect. Moreover, we investigate deformations in Figs.3,4 and 5. And then, we can find that when there is only a steel panel, when there is foam attached to the steel panel, and when there is both foam and leather sheet attached to the steel panel, there are no significant differences in deformations of the steel panel except the third peak with the leather sheet. However, deformations both in the foam and the leather sheet are notably different from those in the steel panel.

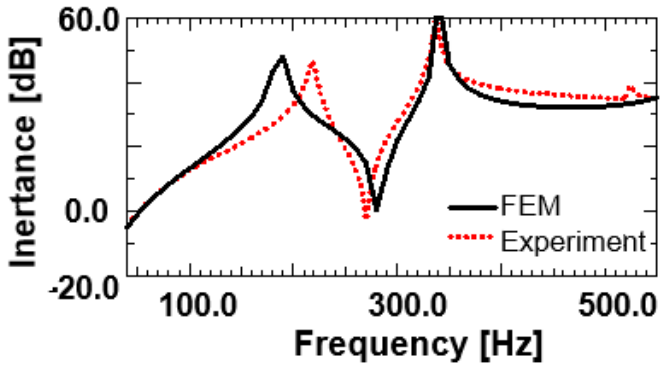

(a) Steel panel

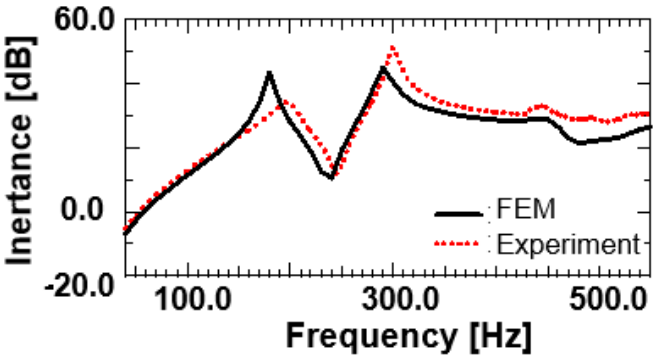

(b) Steel panel with foam

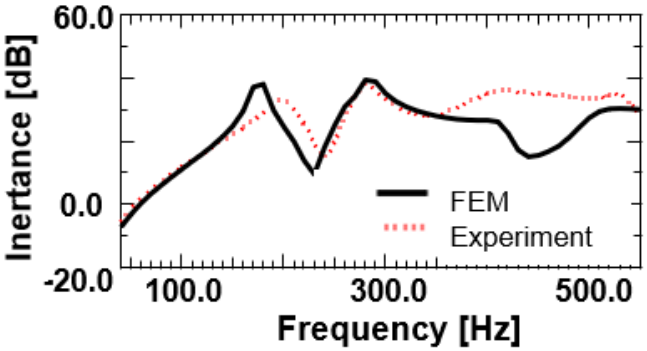

(c) Steel panel with foam and Leather sheet

Fig.2 Frequency Responses

Comparing (b) “Steel with Foam” and (c) “Steel with Foam and Leather” in Fig.2, it can be seen that the presence of the leather sheet slightly lowers the peak level of the inertance transfer function and resonance frequency.

For (a) “Steel” and (b) “Steel with Foam” and (c) “Steel with Foam and Leather”, the deformation distribution of the steel panel in the experiment was reproduced by FEM in Figs.3,4 and 5.

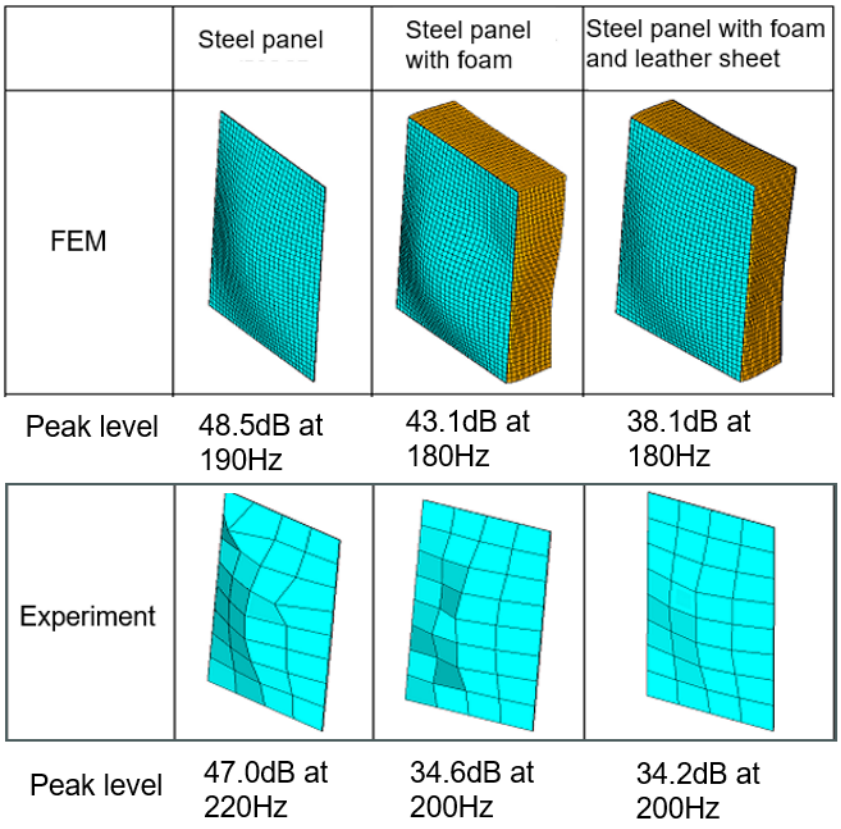

Fig.3 Deformations of 1st peak from hammering test and FEM

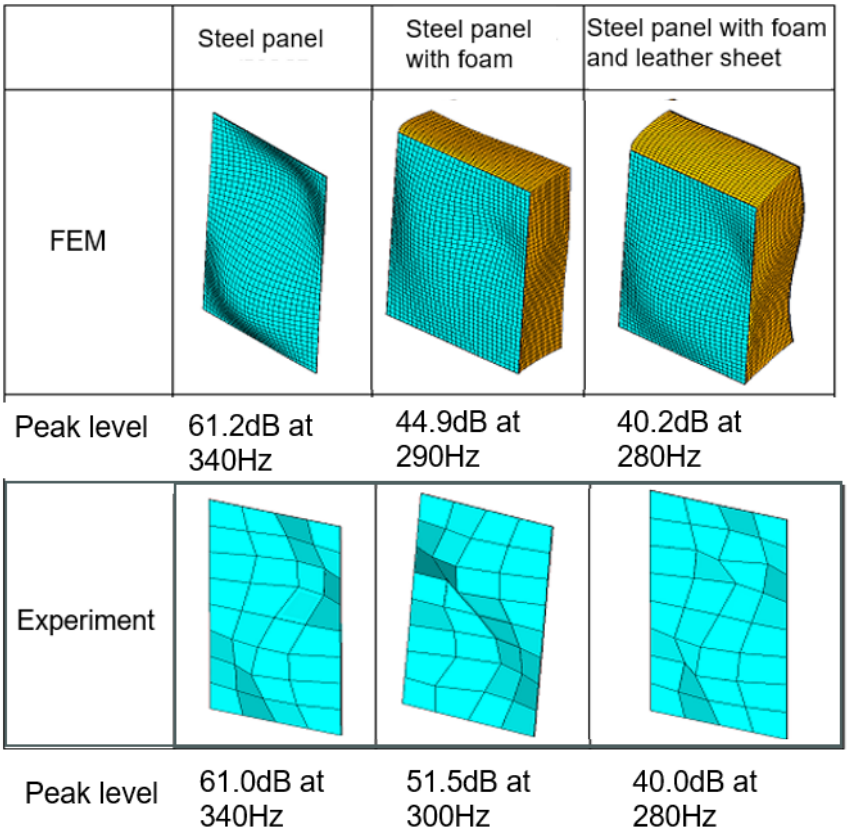

Fig.4 Deformations of 2nd peak from hammering test and FEM

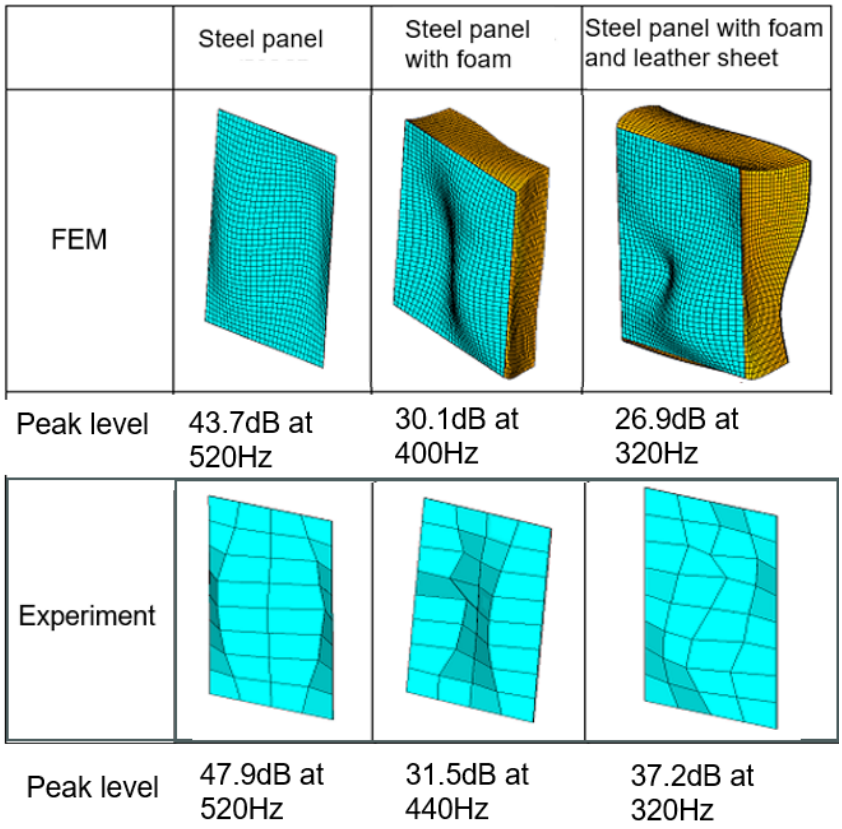

Fig.5 Deformations of the third peak from hammering test and FEM

In Fig.2(c), the FEM calculation responses and experimental responses at the leather's third-order resonance frequency do not match. One reason for this discrepancy between the FEM calculation and experimental results is the heterogeneity of the leather sheet. Actually, the properties of leather sheet vary greatly depending on the part of the animal body, the type of cow, the age, and the sex of the cow. In the FEM analysis for this report, the material properties of the leather sheet specified in the JIS (i.e. Japan Industrial Standards) were used. It will be necessary to measure the material properties of the leather sheet actually used in experiments. And we will use these in the FEM to improve the accuracy of calculation.

In this paper, we reported low frequency vibration characteristics of the rear seat up to 500Hz by the impact force. This frequency range corresponds to structure-borne components for the road noise in the car. In higher frequency, air borne components are governing for the road noise. In this range, the rear seat structures are excited acoustically in general. To evaluate performances in the higher frequency, we will report our next paper.

For our future research work to clarify specific factors quantitatively (e.g., fiber distribution derived from animals or variations in adhesion strength), it may be effective to introduce an internal structure observation using micro-CT scanning and so on. And it will be useful to improve accuracy of the computation that we will adopt the FEM model of the leather as a multilayer anisotropic model. Moreover, we will perform sensitivity analysis to investigate effects of the parameters in detail.

And using the results for the seat in this paper, we will try to perform whole vehicle CAE by linking our previous numerical calculation for the vibration suppression structures around floor panels in the future.

It is of importance to carry out sensitivity analysis of the Biot parameters to clarify the effects of these parameters on the responses. In our future work, we will carry out the sensitivity analysis of these parameters.

It will also be important to carry out numerical analysis in consideration of temperature and humidity- dependent variations in Biot parameters to evaluate vibration characteristics in cars under many environmental conditions. We will try this investigation as our future work.

5. Conclusion

(1) The porous Urethane foam used in the automotive rear seats has the effect of suppressing the vibration of the steel panel backside of the foam used in the automotive rear seat structure. In addition, because of the leather sheets of the seats attached on their surface, a slight damping effect was observed.

(2) We found that when there was only a steel panel, when there was foam attached to the steel panel, and when there was both foam and leather sheet attached to the steel panel, no significant differences in deformations appeared in the steel panel. However, deformations both in the foam and the leather sheet were notably different from those in the steel panel.

(3) By using internal particle displacement and displacement of skeleton as unknowns of FEM for Biot-type poroelastic material, the calculation results of the response analysis were in good agreement with the experimental results. And the deformation distribution of the steel panel with the seat foam having the leather sheet in the experiment was able to be reproduced by FEM.

References

[1] M. A. Biot, “Theory of Propagation of Elastic Waves in a Fluid-saturated Porous Solid (Ⅱ. Higher frequency Range)”, ***Journal of the Acoustical Society of America***, Vol.28, pp.179-191, 1956.

[2] Y. J. Kang and S. Bolton, “A Finite Element Model for Sound Transmission through Foam-lined Double Panel Structures”, ***Journal of the Acoustical Society of America***, Vol.99, pp.2755-2765, 1996.

[3] T. Yamaguchi, T. Fukushima, T. Yamamoto, M. Fujimoto and I. Shirota, "Vibro-acoustic FEA for an Effect of a Sail in Automotive Seat Structures Including Poroelastic Materials and Metal Frames, ***Journal of Technology and Social Science***, Vol.1, No.3, pp. 75-82, 2017.

[4] N. Attala, "A Mixed Displacement-pressure Formulation for Poroelastic Materials" ***Journal of the Acoustical Society of America***, Vol.104, pp.1444-1452, 1998.

[5] T. Yamaguchi, Y. Kurosawa and S. Matsumura, "FEA for damping of structures having elastic bodies, viscoelastic bodies, porous media and gas", ***Mechanical Systems and Signal Processing***, Vol.21, No.1, pp.535-552, 2007.

[6] T. Yamaguchi, Y. Nakamoto, Y. Kurosawa and S. Matsumura, "Dynamic analysis of dissipated energy for automotive sound-proof structures including elastic body, viscoelastic body and porous body using FEM in sound bridge phenomena", ***Journal of Environment and Engineering***, Vol.2, No.2, pp. 315-326, 2007.

[7] T. Yamaguchi, Y. Kurosawa and H. Enomoto, "Damped vibration analysis using finite element method with approximated modal damping for automotive double walls with a porous material", ***Journal of Sound and Vibration***, Vol.325, pp.436-450, 2009.

[8] H. Utsuno, T. W. Wu, A. F. Seybert and T. Tanaka, "Prediction of sound fields in cavities with sound absorbing materials", ***AIAA Journal***, Vol.28, No.11, pp.1870-1875. 1990

[9] O. C. Zienkierwicz and Y. K. Cheung, ***The Finite Element Method in Structural and Continuum Mechanics***, McGraw-Hill, 1967.